Light Metals 2015
Edited by: Margaret Hyland
TMS (The Minerals, Metals & Materials Society), 2015

WETTING BETWEEN CARBON AND CRYOLITIC MELTS. PART I: THEORY AND EQUIPMENT

Ana Maria Martinez [1], Ove Paulsen [1], Asbjørn Solheim [1], Henrik Gudbrandsen [1], and Ingo Eick [2]

[1] SINTEF Materials and Chemistry, Trondheim, Norway, [2] Hydro Aluminium, Neuss, Germany

Keywords: Surface Properties; Wetting; Carbon; Cryolite

Abstract

Several features in the aluminium electrolysis depend on wetting between anode carbon and bath, such as bubble size, gas coverage at the anode, "bubble overvoltage", and the conditions during anode effect. The present paper describes the relevant theory concerning wetting, and factors concerning the choice of method of measurement are discussed. The selected method is based on the immersion-emersion technique, which was adapted for use at high temperature and presence of fluorides, and with polarisation of the sample. The method is based on continuous monitoring of the force acting on a sample which moves into or out from a liquid. There are no restrictions concerning the state of the solid surface. The preferred type of sample is shaped as an inverted cup with thin walls to minimise the ratio between buoyancy and surface tension force. The method was tested using different combinations of solids and liquids at room temperature.

Introduction

Detailed understanding of interfaces is of significant importance for many manufacturing industries, since processes control as well as product quality is affected by interfacial phenomena. A wide range of interfacial phenomena is encountered in high temperature processes, such as Marangoni flow, wettability (contact angle), emulsification, foam formation, jets, and surface waves [1].

In the aluminium electrolysis, wetting between the bath and the anode contributes in determining important properties such as the bubble size, the gas coverage at the anode (area fraction), and the extra ohmic resistance due to the presence of bubbles. Convection in the bath is mainly caused by gas bubbles, which means that wetting will eventually also influence the alumina distribution and the current efficiency. Furthermore, wetting – or more precisely, de-wetting – is involved in the anode effect.

Wetting is also important at the cathode. If there is a bath film present between the metal and cathode carbon, there has to be better wetting between bath and carbon than between metal and carbon. Deterioration of the cell lining is caused mainly by percolation of fluorides through pores in the cathode carbon. This seems to be initiated by sodium, increasing the wetting properties between the melt and the carbon in such a way that the carbon can be fully penetrated in short time [2]. The drained cathode approach relies on finding a material where the metal is present as a film rather than droplets.

The motivation for the present work was to develop a reliable method for measuring contact angles between metal or bath and different materials in the presence of cryolitic melts. Once such a method has been established, it can be used as a tool for selecting better materials, *e.g.*, lining materials for less degradation, or qualification of candidate cathode materials. In addition, better fundamental understanding of the behaviour of the gas bubbles at the anode might be expected.

The present paper mainly describes the theory concerning wetting, the selected method, and some results obtained during testing of the equipment.

Theory and Methods of Measurements

Surface Tension and Wetting Angle

The term wettability can be defined as the tendency of a fluid to spread preferentially onto or adhere to a solid surface in the presence of two immiscible fluids. The surface tension (σ), which is normally expressed in Nm^{-1}, can be related to the work required to create a unit area of the surface ($Jm^{-2} = Nm^{-1}$). All surfaces have a certain surface tension. The contact angle (contact angle) θ at a three-phase boundary (triple line) can be related to these surface tensions by Young's equation (see Figure 1),

$$\cos\theta = \frac{\sigma_{sg} - \sigma_{sl}}{\sigma_{lg}} \qquad (1)$$

The contact angle is always measured through the liquid. If $\sigma_{sg} < (\sigma_{sl} + \sigma_{lg})$, the droplet will spread out on the surface to form a film, while the gas bubble takes the shape of a sphere (neglecting gravity). On the other hand, if $\sigma_{sl} < (\sigma_{sg} + \sigma_{lg})$, a gas film will be formed underneath the solid.

The equilibrium wetting angle will be influenced by chemical heterogeneity and bubble surface contamination as well as solid surface roughness.

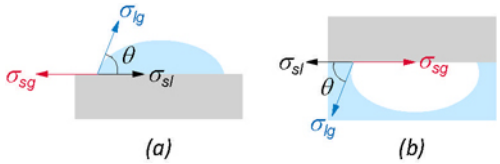

Figure 1. Balance between forces at the three-phase boundary between solid, liquid, and gas. a) – droplet resting on the solid, b) – gas bubble underneath the solid.

Wetting Hysteresis

Most real processes involving wetting are hysteretic or energy-dissipating. Despite that the dynamic (hysteretic) wetting behaviour is often more interesting than the equilibrium situation, the literature on dynamic behaviour is comparatively scarce.

Wetting hysteresis (contact angle hysteresis) can be defined as the change in wetting angle due to motion of the triple line along the solid surface; see Figure 2. The advancing contact angle (θ_a) can be defined as the contact angle at the location where the gas phase is displaced by the liquid. The receding contact angle (θ_r) is then defined as the contact angle at the location where the liquid is being replaced by gas. Note that this definition involves that the advancing angle will be at the front of a droplet, but at the trailing part of a bubble.

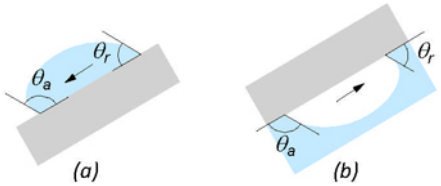

Figure 2. Advancing and receding angles of wetting for a droplet (a) and a gas bubble (b).

In the case of solid-liquid contacts, hysteresis has usually been attributed to surface roughness or chemical heterogeneity, although significant hysteresis has been reported on molecularly smooth chemically homogeneous surfaces [3]. According to Chen *et al.* [4], the most important mechanisms that can give rise to hysteresis are, i) mechanical hysteresis, arising from intrinsic mechanical irreversibility of many adhesion/de-cohesion processes, and ii) chemical hysteresis, arising from the intrinsic chemical irreversibility at the surfaces associated with rearrangement of chemical groups. The latter means that the solid surface is not necessarily the same just before it becomes covered by liquid as just after the liquid has left the surface.

Methods of Measurement

A comprehensive description of different methods for measuring contact angles is given by Deyev and Deyev [5]. The "best" method depends on the nature of the surface, and some of the methods are difficult to apply at high temperature. Most methods described in the literature are variants of the sessile drop technique, capillary displacement, or the immersion-emersion technique.

When using *the sessile drop technique*, the experiment consists essentially of permitting a drop of liquid to spread onto a horizontal solid substrate until equilibrium is achieved. Contact angles (θ) and liquid surface energies (σ_{lg}) can be calculated from the shape of the drop as derived from photography. Although the method is simple in principle, the equipment tends to be expensive due to the requirements concerning quality of surfaces and optics.

Dynamic capillary displacement is based on the classic capillary rise experiment. The contact angle is determined by measuring the distance a liquid is raised or depressed above or below the external liquid surface. The method has been applied for wetting studies at low as well as high temperatures.

The *"spot technique"* reported by Awasthi et al. [6] is based on a well-standardized method for obtaining melting points. The method makes use of the high reflectivity of the liquid metal surface which acts as a mirror. The metal is kept in a heated inert cup, and the shape of a liquid metal, which is a function of the wetting angle, is measured.

An *electrolysis cell* for predicting the wettability of aluminium on cathode materials was described in a US Patent from 1979 [7]. The idea is to use a small electrolysis cell, and the size of the largest aluminium droplets is used as a measure of the wetting properties.

The *immersion-emersion technique* ("wetting balance") was selected for the present purpose, and this method will be described more thoroughly in the following.

The Immersion-Emersion Technique

The apparatus described in the present paper was based on the immersion-emersion technique. This method was considered to be the only method that could fulfil all the requirements,

- Possibility of measuring at high temperature and in presence of fluoride vapour
- Possibility of measuring at dynamic conditions
- Possibility of measuring during polarisation
- No restrictions on the state of the solid surface, *e.g.*, smoothness

Basically, the method is a variant of the maximum pull (or detachment) method used to measure liquid-vapour surface tensions. The method is commonly used in the electronics industry to quantify wetting of solders, but it has also been used for wetting studies in metal-ceramic systems [8].

The method consists of continuously monitoring the force acting on a solid which moves into or out from a liquid during an immersion-emersion circle. The advancing contact angle is obtained during immersion, while the receding angle is measured during emersion; see Figure 3. If the contact angle is below 90 ° it can be measured by optically (since the liquid meniscus formed around the solid is above the horizontal flat liquid surface) or by tensiometry. For wetting angles higher than 90°, tensiometry is the only option.

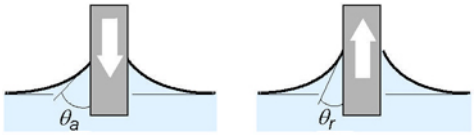

Figure 3. Meniscus formed around a solid during immersion and during emersion. The advancing wetting angle (θ_a) is usually larger than the receding angle (θ_r).

Tensiometry. Buoyancy Correction

By tensiometry, the total weight of the solid body is measured as it undergoes an immersion-emersion cycle. The total weight is made up of three terms, i) the weight of the solid body in gas (m_0), ii) the byouancy of the immersed part of the body (m_b), and iii) the weight of the meniscus (m_σ).

The governing equation in tensiometry is

$$F = L \cdot \sigma \cdot \cos\theta \quad [N] \qquad (2)$$

where F is the force acting on the solid body in the vertical direction, L is the length of the meniscus [m], and σ is the surface tension between liquid and gas [Nm^{-1}]. The measured weight due to the surface tension becomes

$$m_\sigma = F/g \quad [kg] \qquad (3)$$

This weight corresponds exactly to the weight of the liquid lifted above the general liquid level far from the body (represented by the dotted line in Figure 3). The buoyancy term is given by

$$m_b = Ah\rho_l \quad [kg] \tag{4}$$

where A is the cross-sectional area of the body [m^2] and h is its immersion depth [m] (below the general liquid level indicated by the dotted line in Figure 3). Since the immersion depth changes linearly with time during the measurement, the buoyancy term also varies with the time.

Viscous stress on the main part of the plate can be neglected when the dimensionless capillary number Ca << 1;

$$Ca = \frac{\mu u}{\sigma} \tag{5}$$

where μ is the viscosity of the liquid [$kgm^{-1}s^{-1}$] and u is the characteristic velocity [ms^{-1}] (here, the rate of immersion or emersion). The maximum velocity used in the present work was 1 mm/s, which gives Ca ≈ 10^{-5}. Still, it cannot be excluded that the difference between the equilibrium wetting angle and the dynamic angles are partly caused by viscous deformation of the meniscus close to the triple line [9].

Description of the Apparatus

The core of the measuring equipment is,

- A carbon crucible or a beaker containing the liquid
- A sample (usually shaped as an inverted cup) suspended from a load cell
- A linear actuator driven by a stepping motor for moving the crucible up and down

A cross-section of the graphite crucible and a carbon sample is shown in Figure 4. The crucible was mounted on a graphite supporter and connected to the actuator (IAI ROBO Cylinder RCP2 Series, ±0.02 mm repeatability) by a 12 mm diameter stainless steel rod. The crucible was fitted inside a vertical gas tight tube-type laboratory furnace lined with a 100 mm dia. x 700 mm length mullite tube. The furnace was equipped with water cooled stainless steel end closures with O-ring seals between the steel part and the ceramic tube (Figure 5).

The load cell was of type FUTEK LSB200 with a load capacity of 22 N and temperature compensated up to 72 °C. The cell was fitted inside a water-cooled gas tight chamber flushed with argon on top of the furnace. The anode samples (some are shown in Figure 6) were connected to a threaded steel tube which in turn was suspended from the load cell by means of a platinum wire. The sample assembly was electrically insulated from the load cell. For running experiments during electrolysis, DC current could be run through the anode sample. The power supply was provided via one or two flexible copper wires connected to the steel tube holding the anode sample as shown in Figure 7. An extra weight was placed at the top of the sample to ensure that it was absolutely perpendicular (not shown in the figure). To prevent over-heating of the load cell and the electrical wiring, several heat shields of stainless steel was placed between the anode sample and the load cell chamber. By the combination of water cooling and heat shields the temperature in the load cell chamber was kept below 40 °C during the wetting experiments. The temperature was measured by a type S thermocouple placed close to the graphite crucible containing the electrolyte. The signal from the load cell was logged via a FUTEK IPM650 microcontroller which has a 24 bit A/D converter, with a non-linearity better than 0.001%, high noise suppression, and low temperature coefficient.

The sampling frequency was usually 5 s^{-1}.

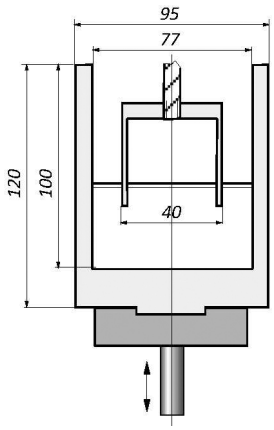

Figure 4. Graphite crucible, graphite supporter, and carbon sample.

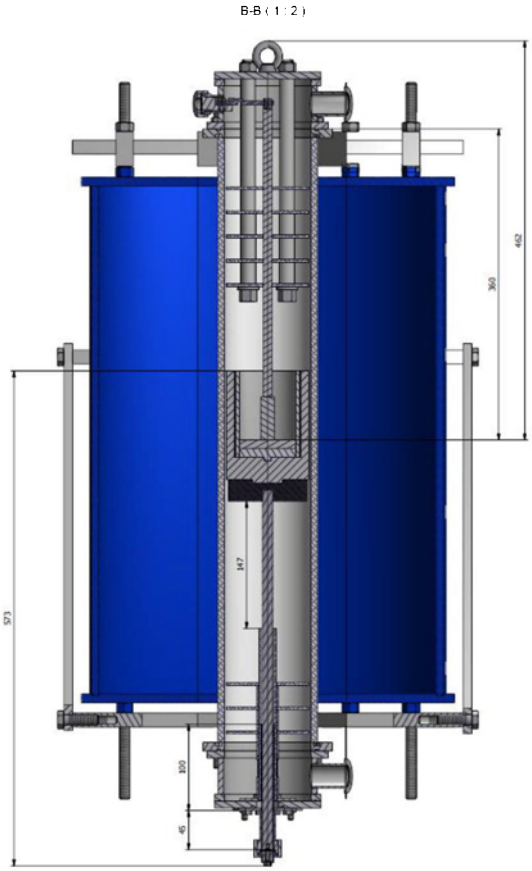

Figure 5. Cross-section through the laboratory furnace.

Figure 6. Anode carbon samples with 40 mm external diameter and 2.5 mm, 5 mm, and 10 mm wall thicknesses.

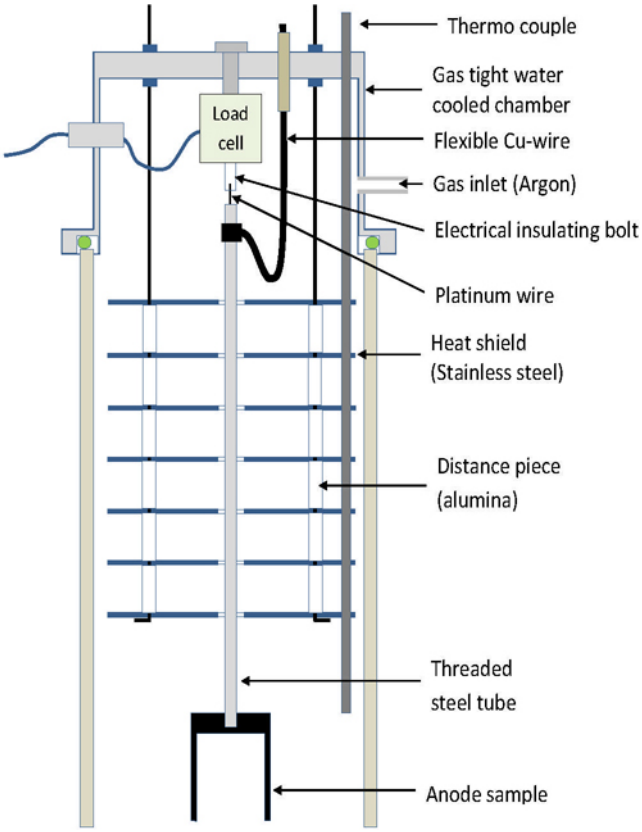

Figure 7. The upper half of the experimental setup with load cell, anode sample, thermocouple and DC powder for running experiment during electrolysis. The crucible with the electrolyte is not shown.

Test of Equipment

The equipment was tested by performing measurements at room temperature, with either water or ethanol/water as liquid and quartz or copper as the solid material. Since the main purpose was to gain some experience in treating the data and to see that all parts of the equipment worked properly, no special care was taken in cleaning and pre-treatment of the samples besides rinsing them with ethanol and distilled water.

Experimental

The test specimen had similar shape and dimensions as the thin-walled carbon sample shown in Figure 7. The quartz sample was made of a 40 x 37 mm diameter tube. The theoretical surface tension force with the given dimensions and data for water (σ = 0.07305 Nm^{-1} at 18 °C [10]) becomes 0.0177 N (corresponding to 1.80 g) at full wetting (θ = 0°, see Equation (2)). The ethanol-water mixture contained 60 vol% ethanol and had a surface tension of 0.027 Nm^{-1} [10]. The copper probe was made from a foil shaped by wrapping it around a 37.8 mm diameter plastic tube. The probes were suspended in a platinum wire and the liquid was kept in a beaker glass with same dimensions as the crucible shown in Figure 4 for visual inspection. The beaker glass was moved up or down at 1 mm/s.

Treatment of Data

The raw data comprises the weight and the position of the beaker glass or crucible, recorded with a sampling frequency of 5 Hz.

Figure 8 shows the recorded weight mass in the system water-quartz as a function of the beaker glass position. The theoretical weight in the absence of surface tension forces is also shown (effect of buoyancy). As can be observed, there is a considerably hysteresis in the curve, reflecting the difference between the advancing contact angle (when the beaker glass is being lifted) and the receding contact angle (when the beaker glass is lowered).

The difference between the recorded weight (m_m) and the theoretical weight (m_t) was plotted as a function of the position; see Figure 9. The average differences in the position range 15-32 mm are represented by red lines. These weights correspond to the receding and the advancing wetting angles, as indicated in the figure.

The recorded lines were not straight in this case. Possibly, this can be attributed to the condition of the quarts glass surface; it can be suggested that small disturbances, even a small finger mark, is sufficient to disturb the measurements.

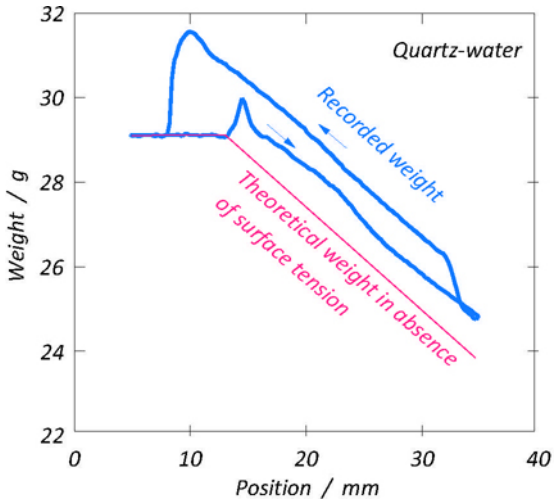

Figure 8. Recorded weight and theoretical weight in absence of surface tension (only buoyancy taken into consideration) as a function of the beaker glass position. System: Quartz-water.

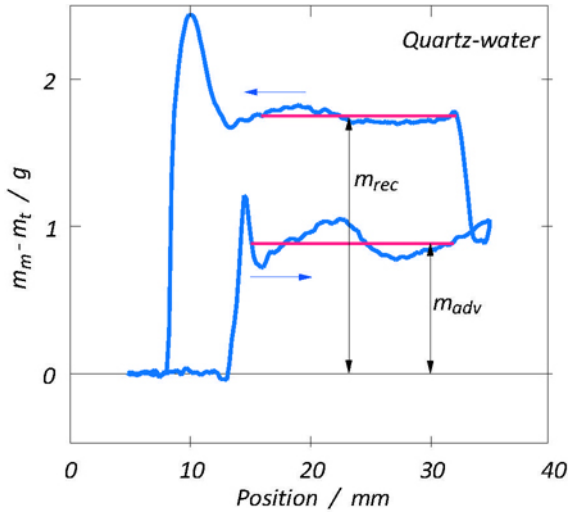

Figure 9. Difference between the recorded weight (m_m) and the weight (m_t) in absence for surface forces (Figure 8) as a function of the position. The subscripts "rec" and "adv" refer to receding and advancing wetting angles, respectively.

Results and Discussion

Plots showing the difference between the recorded and theoretical weights for the systems copper-water, quartz-ethanol, and copper-ethanol are shown in Figs. 10-12. The results are summarized in Table 1. As can be observed, there are generally quite large differences between the advancing and the receding wetting angles, except for copper-ethanol.

According to Sumner *et al.* [11], the equilibrium wetting angle for the system quartz-water is 22 °, which is between the advancing and receding angles shown in Table 1. Sikalo *et al.* [12] found advancing wetting angles of 10 ° and 78 ° for smooth and rough glass, respectively, while the receding angles were 6 ° (smooth glass) and 16 ° (rough glass). The type of glass was not specified.

Fan *et al.* [13] studied equilibrium wetting angles between mixtures of water and ethanol and different metals. For copper-water the wetting angle was given to be 100 °, which is close to the advancing angle given in Table 1.

For copper-60% ethanol, the data by Fan *et al.* [13] indicates about 30 ° (as read from a graph). This fits very well with our data.

No data were found for the system quartz-60% ethanol. This system showed a very strange behaviour, since the advancing wetting angle was smaller than the receding angle. The reason for this behaviour is not clear, but it must be related to the conditions at the surface. A probable reason is adsorption and desorption processes taking place at the meniscus as the sample is moved through the liquid. Another possibility is the effect of evaporation of ethanol at the meniscus, which causes locally increased surface tension and surface-driven flow (this is the mechanism for formation of droplets on the inner walls of a cognac glass).

A number of measurements using a ceramic plate and different mixtures of water and ethanol consistently showed the same behaviour. To the authors' best knowledge, smaller advancing wetting angle than receding wetting angle has not been reported earlier in the literature.

The local peak at the beginning of immersion and ending of emersion in some of the experiments is probably caused by slightly uneven orientation of the sample. At the first contact point the liquid is completing up the wetting of the bottom ring, even if it is partly slightly above the liquid level, resulting in a weight peak. When emerging the liquid the same process occurred backwards, resulting in another weight peak. In the "hot" measurements involving cryolitic melts, great efforts were made in placing the bottom of the sample horizontal.

From the results obtained, it was concluded that the apparatus was functioning satisfactorily. Results obtained with carbon and cryolitic bath will be presented in Part II of this work [14].

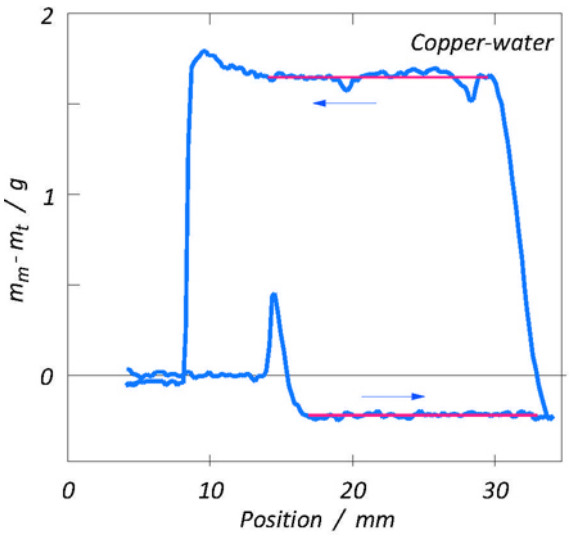

Figure 10. Difference between the recorded weight (m_m) and the theoretical weight (m_t) as a function of the position for the system copper-water.

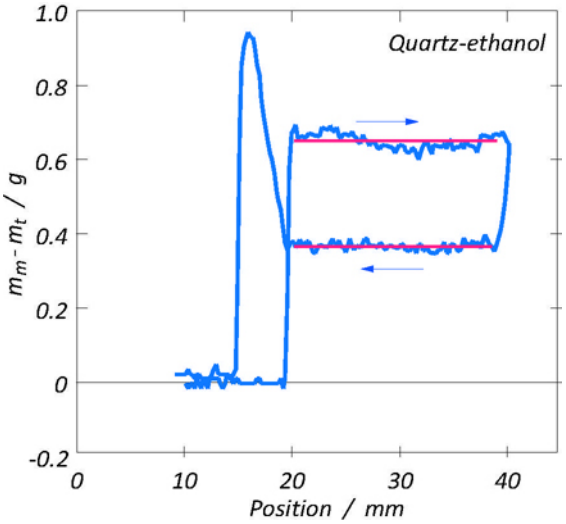

Figure 11. Difference between the recorded weight (m_m) and the theoretical weight (m_t) as a function of the position for the system quartz-ethanol. Please note that the advancing contact angle appears to be smaller than the receding angle.

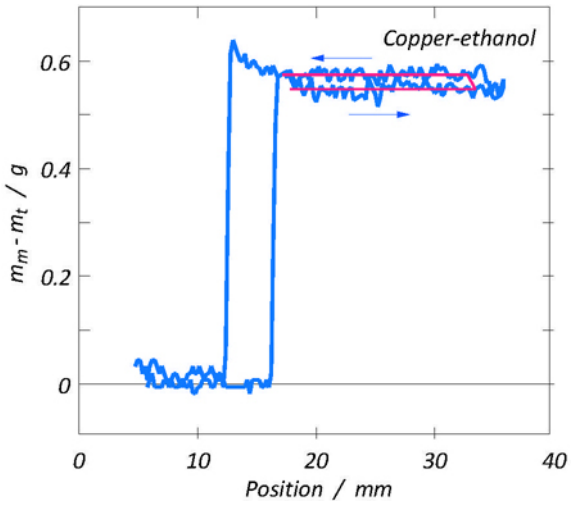

Figure 12. Difference between the recorded weight (m_m) and the theoretical weight (m_t) as a function of the position for the system quartz-ethanol.

Table 1. Calculated advancing and receding angles of wetting (θ).

System	Direction	θ [°]
Quartz/water	Receding	10.3
	Advancing	60.2
Copper/water	Receding	21.1
	Advancing	97.2
Quartz/ethanol	Receding	56.0
	Advancing	7.6
Copper/ethanol	Receding	28.4
	Advancing	33.0

Acknowledgement

The present work was supported by the HAL Ultra Fundamental projects financed by the Research Council of Norway and Hydro Aluminium. Permission to publish the results is gratefully acknowledged.

References

1. K.C. Mills, E.D. Hondros and Z. Li, "Interfacial Phenomena in High Temperature Processes", *Journal of Materials Science*, **40** (2005), pp. 2403/9.
2. K. Tschöpe, A. Støre, S. Rørvik, A. Solheim, E. Skybakmoen, T. Grande, and A.P. Ratvik, "Investigation of the Cathode Wear Mechanism in a Laboratory Test Cell", Light Metals 2012, pp. 1349/54.
3. A.M. Schwartz, "Contact angle hysteresis: A molecular interpretation", *Journal of Colloid and Interface Chemistry*, **75** (2) (1980), pp. 404/8.
4. Y.L. Chen, C.A. Helm and J.N. Israelachvili, "Molecular Mechanisms Associated with Adhesion and Contact Angle Hysteresis of Monolayer Surfaces", *Journal of Physical Chemistry*, **95** (1991), pp. 10736/47.
5. G. Deyev and D. Deyev (Eds.), Surface Phenomena in Fusion Welding Processes, CRC Press (2006).
6. A. Awasthi, Y.J. Bhatt, and S.P. Garg, "Measurement of Contact Angle in Systems Involving Liquid Metals", *Measurement Science and Technology*, **7** (1996), pp. 753/7.
7. S. K. Das, "Controlled wettability graphite electrodes for selective use in electrolysis cells", US Patent 4,179,345 (1979).
8. I. Rivollet, D. Chatain, and N. Eustathopoulos, "Simultaneous Measurement of Contact Angles and Work of Adhesion in Metal-Ceramic Systems by the Immersion-Emersion Technique", *Journal of Materials Science*, **25** (1990), pp. 3179/85.
9. E. Ramé, "The Interpretation of Dynamic Contact Angles Measured by the Wilhelmy Plate Method", *Journal of Colloid and Interface Science*, **185** (1997), pp. 245/51.
10. R.C. Weast (ed.), CRC Handbook of Chemistry and Physics, 66th Edition 1986, CRC Press, Inc.
11. A.L. Sumner, E.J. Menke, Y. Dubowski, J.T. Newberg, R.M. Penner, J.C. Hemminger, L.M. Wingen, T. Brauersc, and B.J. Finlayson-Pitts, "The Nature of Water on Surfaces of Laboratory Systems and Implications for Heterogeneous Chemistry in the Troposphere", *Phys. Chem. Chem. Phys.*, **6**, (2004), pp. 604/13.
12. S. Sikalo, M. Marengo, C. Tropea, and E.N. Ganic, "Analysis of Impact of Droplets on Horizontal Surfaces", *Experimental Thermal and Fluid Science*, **25** (2002), pp. 503/10.
13. L. Fan, X. Yuan, C. Zhou, A. Zeng, K.-T. Yu, M. Kalbassi, and K. Porter, "Contact Angle of Ethanol and n-Propanol Aqueous Solutions on Metal Surfaces", *Chem. Eng. Technol.*, **34** (9) (2011), pp. 1535/42.
14. A. Solheim, H. Gudbrandsen, A.M. Martinez, K.E. Einarsrud, and I. Eick, "Wetting between Carbon and Cryolitic Melts. Part II: Effect of Bath Properties and Polarisation", Light Metals 2015 (This volume).